AIAA JOURNAL
Vol. 31, No. 7, July 1993

Measurements in a Pressure-Driven Three-Dimensional Turbulent Boundary Layer During Development and Decay

Walter R. Schwarz* and Peter Bradshaw†
Stanford University, Stanford, California 94305

Measurements of the turbulence structure in the outer layer of a three-dimensional turbulent boundary layer were made in an open-circuit low-speed blower tunnel. The three-dimensional turbulent boundary layer on the floor of the tunnel was generated by a cross-stream pressure gradient using a 30-deg bend in the horizontal plane. Downstream of the bend, the three-dimensional turbulent boundary layer gradually relaxed toward a two-dimensional turbulent boundary layer as the crossflow decayed slowly after the cross-stream pressure gradient was removed. Mean velocities were measured with a three-hole pressure probe, and turbulence quantities, which included the Reynolds-stress tensor and the triple products, were measured with a cross-wire hot-wire anemometer. The experiment provides new data that isolate the effects of crossflow from the effects of an adverse streamwise pressure gradient that may have clouded the interpretations of previous three-dimensional turbulent boundary-layer experiments. Another advance over previous work is that enough turbulence quantities were measured for all terms in the Reynolds-stress transport equations to be evaluated, allowing term-by-term tests of stress-transport turbulence models.

Introduction

MANY flows such as those over swept wings of aircraft and also those inside turbomachines are affected by three-dimensional turbulent boundary layers (TBLs). The aerospace industry's need for turbulence models to apply to these flows is an incentive for studying three-dimensional TBLs. Typically, turbulence models are used in computational fluid dynamics analyses that calculate the expected performance of aircraft designs or the degree of mixing that occurs inside turbomachines. Frequently, turbulence models extended from two-dimensional TBL models are applied to three-dimensional TBLs like these with poor results due to significant changes in turbulence structure.

The mean flowfield of a typical three-dimensional TBL is characterized by having mean velocity vectors nearly parallel to the surface along which the boundary layer grows. However, the directions of the velocity vectors may vary from the direction of the freestream velocity vector. We will use an aircraft wing as an example and define the streamwise (flight direction), normal, and spanwise example and define the streamwise (flight direction), normal, and spanwise directions as x, y, and z with mean velocity components U, V, and W, respectively. We distinguish three-dimensional TBLs from other possible three-dimensional shear flows, such as imbedded longitudinal vortices, by the smallness of V compared with U and/or W, analogous to the definition of a two-dimensional TBL except that W is the same order as U.

The notable difference between three-dimensional and two-dimensional TBLs is the presence of the mean velocity gradient $\partial W/\partial y$. This additional mean velocity gradient is the main part of the axial vorticity in the three-dimensional TBL, $\partial V/\partial z$ being small via the boundary-layer approximation. Also, $\partial W/\partial y$ contributes to the production terms for some Reynolds stresses, especially the y-z plane shear stress $-\rho\overline{vw}$.

Many previous three-dimensional TBL experiments in various geometries have been summarized by Johnston,[1] Fernholz and Vagt,[2] and Anderson and Eaton.[3] Even in 1976, Johnston cited over 80 experiments on three-dimensional TBLs. Our discussion is limited to those experiments in which all components of the Reynolds-stress tensor were measured. All too often, the vital y-z plane shear stress $-\rho\overline{vw}$ has been omitted because it is difficult to measure.

Usually, three-dimensional TBLs result either from shearing forces applied to the fluid by a moving surface or from the application of a cross-stream pressure gradient that deflects the streamlines of the flow close to the surface more strongly than near the freestream. Thus, three-dimensional TBLs are generally referred to as being either shear driven or pressure driven. Here, we do not consider "stress-induced" three-dimensional shear flows (Prandtl's second kind of secondary flow).

Most three-dimensional TBL experiments were flows in which crossflow was imposed on a two-dimensional TBL by a pressure gradient. The experiments of Bradshaw and Terrell,[4] Johnston,[5] Elsenaar and Boelsma,[6] East and Sawyer,[7] and Bradshaw and Pontikos[8] had a spanwise-component flow that approximated untapered swept wings of infinite span ("infinite yawed flows"). Three-dimensional TBLs on the plane endwalls of curved rectangular ducts were studied by Pierce and Duerson[9] and DeGrande and Hirsch.[10] Other experiments on flows approaching obstacles include those of Pierce and Ezekewe,[11], Dechow and Felsch,[12] Müller,[13] and Anderson and Eaton.[3] Fernholz and Vagt[2] studied the three-dimensional TBL in a flow along a circular cylinder that approached separation moving toward a slanted back plate in a wind tunnel.

The shear-driven three-dimensional TBL experiments, which typically involve flow along a rotating cylinder, include those of Bissonnette and Mellor,[14] Lohmann,[15] Driver and Hebbar,[16] and Driver and Johnston.[17] Another approach, used by Littell and Eaton,[18] was to generate a three-dimensional TBL on a spinning disk. The shear drove the circumferential motion, and the circumferential motion provided the "centrifugal force" to drive the crossflow in the radial direction. Direct numerical simulations (full time-dependent Navier-Stokes solutions) are now being widely used to obtain

Received Sept. 26, 1992; revision received Nov. 25, 1992; accepted for publication Nov. 27, 1992; presented as Paper 93-0543 at the AIAA 31st Aerospace Sciences Meeting, Reno, NV, Jan. 11-14, 1993.

*Research Assistant; currently Assistant Professor, Department of Mechanical Engineering, Stevens Institute of Technology, Hoboken, NJ 07030.

†Thomas V. Jones Professor of Engineering, Department of Mechanical Engineering.

the same types of information provided by traditional experiments and to supply data for quantities that are difficult or impossible to measure. Recent direct numerical simulations of three-dimensional TBLs were performed by Spalart,[19] Moin et al.,[20] and Sendstad and Moin.[21]

Previous experiments have provided no consensus on whether the shear-stress vector always lags, or sometimes leads, the velocity-gradient vector, but it is generally agreed that they do not coincide. The directions of the shear-stress vector and velocity-gradient vector can be defined as

$$\gamma_\tau \equiv \tan^{-1}\left(\frac{\overline{vw}}{\overline{uv}}\right) \quad \text{and} \quad \gamma_g \equiv \tan^{-1}\left[\frac{(\partial W/\partial y)}{(\partial U/\partial y)}\right] \tag{1}$$

The difference between them indicates that simple eddy-viscosity models are not appropriate in these types of flows: isotropic eddy viscosity would imply $\gamma_\tau = \gamma_g$. It is found that γ_τ usually lags behind γ_g as the latter increases with x. Opposite trends were seen by Lohmann,[15] Pierce and Ezekewe,[11] Fernholz and Vagt,[2] Müller,[13] and Driver and Hebbar.[16]

Another quantity used to identify departure from simple isotropic eddy viscosity is the eddy-viscosity ratio

$$N_e = \tan(\gamma_\tau - \gamma_u)/\tan(\gamma_g - \gamma_u) \tag{2}$$

where $\gamma_u \equiv \tan^{-1}(W/U)$ and $N_e = 1$ corresponds to isotropic eddy viscosity. In many three-dimensional TBL experiments, N_e has been observed to differ significantly from 1.

It is also frequently observed that the ratio of turbulent shear stress to twice the turbulent kinetic energy (TKE),

$$a_1 \equiv [(\overline{uv})^2 + (\overline{vw})^2]^{1/2}/\overline{q^2} \tag{3}$$

decreases in the presence of crossflow. The a_1 parameter can be crudely regarded as the efficiency of the eddies in producing turbulent shear stresses for a given amount of TKE. Some investigators have found that the decrease in a_1 is simply due to a decrease in $-\overline{uv}$ when crossflow is applied to a two-dimensional TBL; however, this is not always the case. In the experiments of Pierce and Duerson,[9] DeGrande and Hirsch,[10] and Anderson and Eaton,[3] the turbulent shear stresses increased in the outer layer. The turbulent shear stresses in the present experiment also increased.

Bradshaw and Pontikos[8] suggested that the reduction in a_1 was attributable to the sideways toppling of large eddies in the presence of a crossflow. The tilting of the large stress-producing eddies in the outer layer results in an orientation in which the production of shear stress by the large eddies is less efficient than it would be in a two-dimensional TBL. Eaton,[22] expanding on earlier work by Anderson and Eaton,[3] explained the reduction in a_1 as the result of changes in the flow structure near the wall. This reduction was hypothesized to be due to the crossflow both decreasing the number of low-speed streaks at the wall and degrading the effects of longitudinal vortices. This explanation may not be relevant to the outer layer.

The objective of the present experiment was to study and explain the changes in turbulence structure that develop due to crossflow in the boundary layer, specifically in the outer layer where these changes appear to be largest. This work included mapping the mean flowfield (velocity magnitude and direction), performing detailed turbulence measurements, determining the surface static pressure distribution, measuring the surface shear stress, and performing surface flow visualization.

The present experiment also provides new data for developing and testing turbulence models for three-dimensional TBLs. Another advance over previous work is that the measurements are detailed enough for all terms in the Reynolds-stress transport equations to be evaluated, either directly or by difference. Our tests of turbulence models for the triple products and the pressure-strain redistribution terms[23] will be reported separately.

The present experiment has a companion experiment by Flack and Johnston[24] that concentrates on the inner layer of a three-dimensional TBL using laser techniques in a water channel. This was a deliberate splitting of the work: in our experiment emphasis was on the outer-layer structure.

Facility and Experimental Techniques

The experiment was conducted in an open-circuit low-speed blower tunnel with a 762 × 762 mm working section. A three-dimensional TBL on the floor of the tunnel was generated by the imposition of a cross-stream pressure gradient using a 30-deg bend in the horizontal plane as shown in Fig. 1. Downstream of the bend, the three-dimensional TBL gradually relaxed toward a two-dimensional TBL as the crossflow decayed slowly after the cross-stream pressure gradient was removed. The flow was an initial two-dimensional TBL perturbed by a slowly decaying streamwise $\partial W/\partial y$ field, created by the 30-deg bend, which permitted the study of response and recovery. A bend provided a rapid increase of $\partial W/\partial y$ while maintaining a relatively small $\partial p/\partial x$ along the centerline of the test section.

The level of freestream turbulence in the tunnel was approximately 0.3%. The boundary layer that was studied grew on the floor of the working section after being forced to become turbulent by a trip wire (1.6-mm diameter) placed at $x = 0$ mm. At the first measurement station, $x = 826$ mm, the boundary layer was two dimensional and had the following parameters: $\delta_{99} = 20.9$ mm, $\theta_{11} = 2.4$ mm, $H_{11} = 1.38$, $c_f = 0.0030$, and $Re_{\theta 11} = 4.1 \times 10^3$ at a freestream velocity of $U_{\text{ref}} = 26.5$m/s. At $x = 1626$ mm, the entrance of the 30-deg bend, the boundary-layer thickness had grown to approximately 30 mm.

Surface flow visualizations using an oil mixture were used to estimate the surface streamline deflection. Black contact paper was attached to the floor, beginning approximately 150 mm before the beginning of the curved section. The mixture combined titanium dioxide powder, kerosene, and oleic acid (used as a dispersant) in the ratio 5:15:1 by volume.

The mean velocity field was obtained using a three-hole pressure probe constructed from three hypodermic tubes (1.4 mm o.d.) with the end tubes chamfered at 35-deg angles as recommended by Bryer and Pankhurst.[25] A near-nulling method, which aligned the probe to within 1 deg of the flow direction, was used. Final resolution of the flow direction was obtained using the probe yaw calibration performed in the freestream. Wall proximity effects were accounted for using a Young and Maas[26] type correction based on the height of the probe in a two-dimensional TBL. This correction was plausible since the probe was nearly aligned with the flow direction. The uncertainty in velocity magnitude was ±0.2 m/s, and the flow direction uncertainty was ± 1 deg.

Surface shear stresses were measured using a Preston tube and Patel's calibration.[27] Although Patel's calibration was developed for a two-dimensional TBL, it was assumed that the law of the wall was valid in three-dimensional TBLs in mild pressure gradients for a distance up to the diameter of the

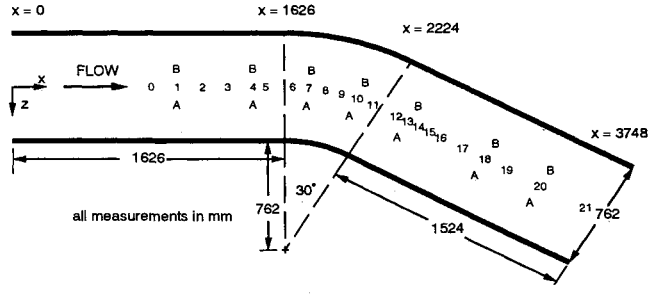

Fig. 1 Plan view of working section showing measurement locations.

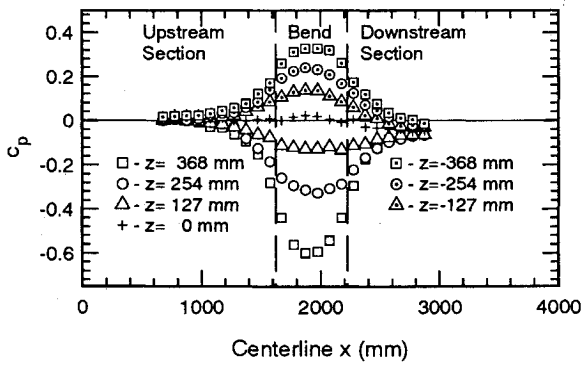

Fig. 2 Static pressure coefficient.

Preston tube. This is consistent with the findings of Pierce et al.[28] and Degani et al.[29] on the existence of near-wall similarity in pressure-driven three-dimensional TBLs. Preston tube measurements were taken with the center tube of the three-hole pressure probe against the floor. The probe was aligned with the mean flow as determined by the three-hole pressure probe near the wall. Extrapolations of the three-hole pressure probe data agreed to within 5 deg of the surface streamline directions obtained with the oil flow visualization.

Turbulence statistics that included the 6 components of the Reynolds-stress tensor, the 10 triple products, and the 3 quadruple products were obtained using a home-built Microscale Systems HWM-100 constant temperature anemometer with a Dantec model 55P51 cross-wire probe. The probe had two platinum-plated tungsten wires with 5-μm diameter and 1.25-mm active length, spaced 1 mm apart and set at angles of approximately ± 45 deg to the flow. The hot-wire fluctuation signals were amplified and low-pass filtered at 30 kHz before being routed to the data acquisition system where the mean and fluctuating signals were separately digitized with 12-bit resolution.

Before each measurement session, the hot wires were calibrated in the freestream to determine the constants for use in the King's law calibration. The effective wire angles were determined using a yaw calibration that was performed once at the beginning of the experiment and then whenever the wires were changed. Turbulence measurements were taken with the plane of the wires placed at four different roll angles. Two of the planes were the U-V and U-W planes. The other two planes were at ± 45 deg to the U-V plane. When placed in the last two planes, the probe was sensitive to $(v + w)/\sqrt{2}$ or $(v - w)/\sqrt{2}$. Statistics involving both v and w fluctuations were determined by combining the signals in the ± 45-deg planes and thus were subject to some additional scatter.

In general, hot-wire measurements are susceptible to a variety of uncertainties that can arise due to calibration, high turbulence intensity, crossflow and prong interference, probe vibration, ambient temperature drift, signal noise, free convection, and wall proximity. The Bearman[30] temperature correction was used to account for ambient temperature drift. The actual temperature variations during a typical 2-h run were less than 3°C. The uncertainties due to crossflow over the hot wires and prong interference were reduced by aligning the probe with the direction of the local mean velocity. Anderson and Eaton[3] quantified the uncertainties in their three-dimensional TBL experiment: they also used Dantec 55P51 cross-wire probes. Their estimated uncertainty values were 5% for $\overline{u^2}$, $\overline{v^2}$, and $\overline{w^2}$; 10% for $\overline{uv}$ and $\overline{vw}$; and 15% for $\overline{vw}$. Measurements in the two-dimensional TBL region of the present experiment agreed within the previous uncertainty values with the Reynolds-stress measurements of Klebanoff[31] and to within 20% of the peak values for the triple products measured by Murlis et al.[32]

Figure 1 shows the 36 measurement locations. The test section was traversed using a system that slid along steel rails mounted on the top of the test section. Different axial positions in the straight test sections were made possible using interchangeable particle board roof panels of varying sizes. One of the roof panels had a slot to allow spanwise traversing without disturbing the roof flow surface. The slot was lined with rubberized foam strips to prevent air leakage through the slot. The roof of the 30-deg bend was made of five 5-deg wedge-shaped Plexiglas panels that had foam-lined slots to allow spanwise (radial) traversing of the probe. Traverses could be made at the 2.5-, 7.5-, 12.5-, 17.5-, 22.5-, and 27.5-deg locations. Once the traverse system had been manually placed in the desired axial position, a microcomputer and stepper motors were used to control vertical, spanwise, yaw, and roll movements. A gooseneck-shaped section of the probe stem inside the tunnel allowed the probe to be yawed without any translation of the probe tip.

The rolling of the probe, necessary to measure all components of the Reynolds-stress tensor, was accomplished with two stepper motors. The cross-wire probe plugged into a Dantec model 55H24 probe support mounted to a shaft rotatable about an axis parallel to the floor. The shaft's angular position was changed by the movement of a control wire loop wrapped around the rotatable shaft and attached to a stepper motor on the probe stem's support platform. The back end of the rotatable shaft connected to a fitting that had eight guide holes. The guide holes provided a means for locking the angular position of the probe, in 45-deg increments, using a spring-loaded pin.

Results of Mean-Flow Measurements

The static pressure was measured at 162 taps in the floor of the test section. Figure 2 shows the distribution of the measured static pressure coefficient

$$c_p \equiv (p - p_{\text{ref}})/\tfrac{1}{2}\rho U_{\text{ref}}^2 \tag{4}$$

throughout the test section. The axial pressure gradient was nearly zero along the centerline until a slight favorable pressure gradient ($0 > \delta\partial c_p/\partial x > -0.01$) developed due to the thickening of the boundary layers in the downstream section. The spanwise pressure gradient was much larger, with a maximum $\delta\partial c_p/\partial z \approx -0.03$ halfway through the bend.

The local skin friction coefficient

$$c_f \equiv \tau_w/\tfrac{1}{2}\rho U_e^2 \tag{5}$$

agreed with that predicted by the two-dimensional TBL correlation[33] $c_f = 0.025 Re_{\theta_{11}}^{-0.25}$ at the first few measurement stations. As the flow entered the bend section, c_f stopped decreasing and maintained a constant value until well into the downstream section. The increased production of turbulent shear stresses in the bend region probably affected the near-wall region and maintained a constant level of wall shear stress.

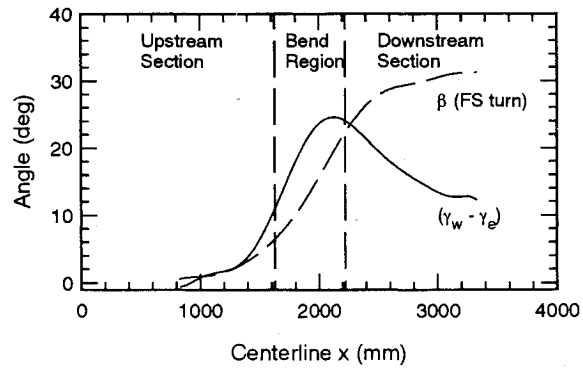

Fig. 3 Crossflow and freestream turning angle.

The crossflow angle $\gamma_u - \gamma_e$ is defined in terms of the directions of the mean velocity vector γ_u and the freestream mean velocity vector γ_e where

$$\gamma_u \equiv \tan^{-1}(W/U), \qquad \gamma_e \equiv \tan^{-1}(W_e/U_e) \tag{6}$$

The axial variation of the maximum crossflow is shown in Fig. 3 along with the turning angle of the freestream β. The slow development of crossflow in the upstream section was followed by a rapid increase in the bend region. The peak crossflow occurred near the exit of the bend region. In the downstream section, the crossflow decreased gradually near the surface but was nearly constant in the outer layer. The behavior of the freestream turning angle in the upstream and bend regions was similar to the growth of the maximum crossflow angle. At the beginning of the downstream section, the rapid increase of the freestream turning angle had ceased and approached 30 deg.

For small turning angles (sin $\beta \approx \beta$, i.e., $\beta < 15$ deg), the inviscid Squire-Winter-Hawthorne (SWH) relationship,[34,35]

$$\frac{U_n}{U_e} = 2\beta\left(1 - \frac{U_s}{U_e}\right) \tag{7}$$

can be used as a rough crossflow model with which to compare the present data. The U_s and U_n are the streamwise and normal velocity components using a coordinate system aligned with the freestream velocity vector, whose magnitude is U_e. The SWH relationship states that the triangular plot of the velocity in the outer region of the boundary layer should have a slope equal to twice the angle β through which the freestream has turned. Using the measured freestream turning angles, the SWH correlation fits the crossflow only in the outer portions of the boundary layer ($y/\delta > 0.5$ approximately) as shown in Fig. 4; closer to the wall, the inviscid approximation is seriously in error.

Results of Turbulence Measurements

These results are presented with respect to a fixed coordinate system aligned with the initial two-dimensional TBL flow. Thus, the x axis is aligned with the upstream tunnel centerline, the z axis is in the spanwise direction, and the y axis is normal to the floor of the test section. This coordinate system shows departures from the initial two-dimensional state of the boundary layer. The sign of the curvature is such that $W > 0$, $\partial W/\partial y < 0$, and $\overline{vw} > 0$ in the outer layer.

In the upstream section, the TKE decreased with axial distance, since it scaled with the square of the friction velocity. Then, as crossflow developed in the bend region, the TKE increased throughout the boundary layer relative to the initial two-dimensional TBL levels. This increase occurred mainly because the crossflow velocity gradient $\partial W/\partial y$ increased production of the Reynolds stresses. A peak in TKE developed at $y/\delta_{99} \approx 0.3$. In the beginning of the downstream section, crossflow decayed slowly and the increased TKE persisted. Later, as crossflow decreased more rapidly, TKE began to decrease. The decrease occurred first at the measurement elevations closest to the wall and then spread outward at locations further downstream. In the outermost part of the boundary layer, the TKE at a given y/δ_{99} was nearly constant as crossflow decayed.

The $-\overline{uv}$ Reynolds stress profiles shown in Fig. 5 behaved similarly to the TKE. The increases in $-\overline{uv}$ resulted mainly from elevated $\overline{v^2}$ values as the crossflow developed. Downstream of the bend, $-\overline{uv}$ decayed. The $\overline{vw}$ values, which were small compared with $-\overline{uv}$, are shown in Fig. 6. Note that since the sense of z has been chosen to make W positive, $\partial W/\partial y$ and the y-z plane shear stress $-\rho\overline{vw}$ are negative except near the surface where W falls to zero. This figure shows the growth of $\overline{vw}$ from zero in the upstream two-dimensional TBL section to values that were approximately 20% of $-\overline{uv}$ where the maximum crossflow occurred. Increases in $\overline{vw}$ were due to the $\overline{v^2}\partial W/\partial y$ generation term. The $-\overline{uw}$ values

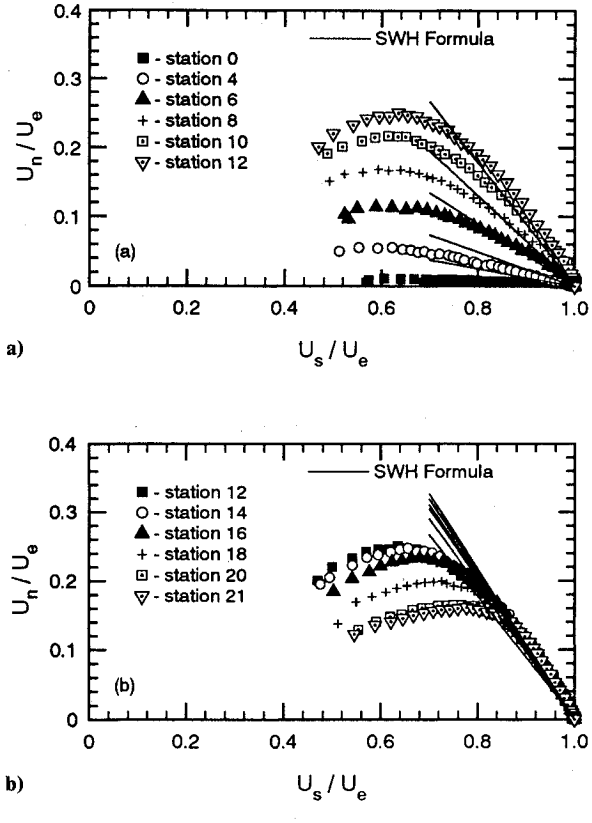

Fig. 4 Triangular plot of velocity: a) crossflow development, b) crossflow decay.

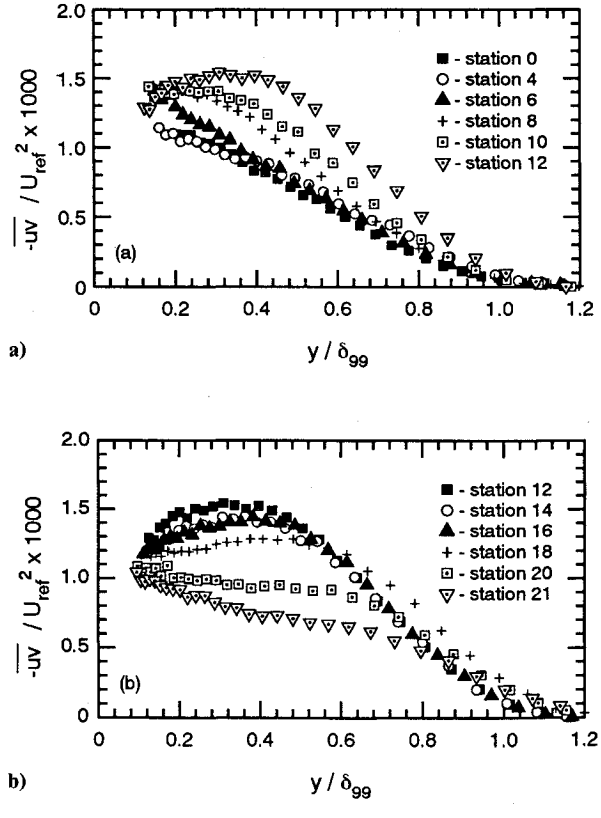

Fig. 5 Profiles of $-\overline{uv}$: a) crossflow development, b) crossflow decay.

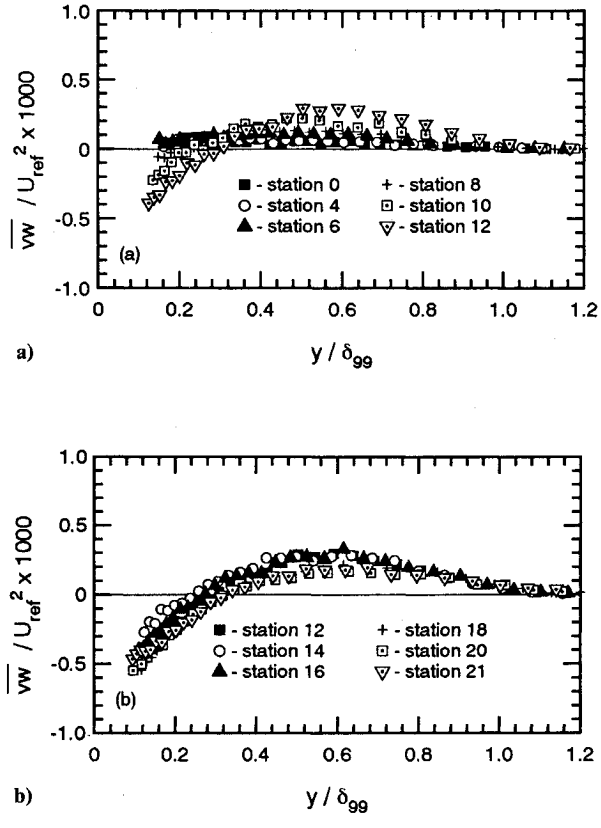

Fig. 6 Profiles of $\overline{vw}$: a) crossflow development, b) crossflow decay.

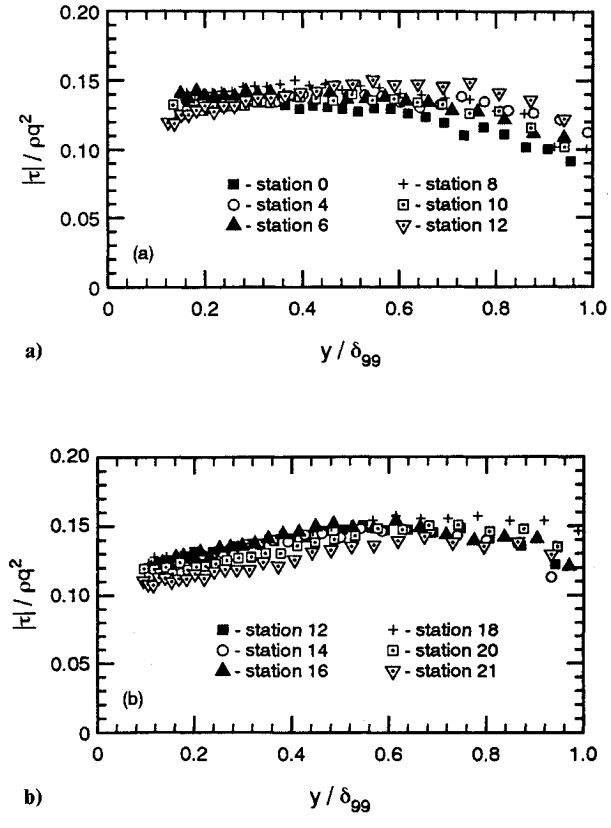

Fig. 7 Profiles of a_1: a) crossflow development, b) crossflow decay.

were negligible in the upstream two-dimensional TBL layer region followed by significant growth of $-\overline{uw}$ in the bend. Downstream of the bend, $-\overline{uw}$ decayed. But $\overline{uw}$ is not important in the transport of either $-\overline{uv}$ or $\overline{vw}$.

In previous three-dimensional TBL experiments, the a_1 parameter [Eq. (4)] decreased below its two-dimensional TBL value. Since most three-dimensional TBL experiments show a_1 to decrease, one might conclude that crossflow is responsible for the decrease; however, the amount of the decrease varies from experiment to experiment. This variation is probably due to the experiments having different degrees of crossflow as well as different streamwise pressure gradient conditions. Since the flow over a swept wing usually experiences a large region of adverse pressure gradient, most of the experiments included adverse pressure gradient conditions.

The presence of an adverse pressure gradient in a two-dimensional TBL was shown by Bradshaw[36] to increase "inactive" motions that can also decrease a_1. Inactive motions do not affect $-\rho\overline{uv}$ (because they do not affect v much). The a_1 parameter decreases because $\overline{u^2}$ and $\overline{w^2}$ increase. In an adverse pressure gradient where the turbulent shear stress decreases near the wall, inactive motion is a larger fraction of $\overline{q^2}$. Thus, considering inactive motion leads to the realization that the behavior of a_1 also depends on pressure gradient.

In this experiment, without any significant adverse streamwise pressure gradient along the centerline, the a_1 parameter displayed in Fig. 7 showed a moderate reduction to approximately 0.12 in the inner half of the boundary layer by the beginning of the downstream test section. In the outer part of the boundary layer, a_1 increased. In the downstream section, as the crossflow slowly decayed, a_1 decreased slightly further.

The eddy-viscosity ratio profiles in Fig. 8 show that N_e reduced to values as low as 0.6 in the crossflow development region and later recovered toward 1.0 as the crossflow decayed. This behavior was intermediate between that of other experiments such as that of Anderson and Eaton,[3] for which N_e decreased to 0.2, and that of Elsenaar and Boelsma,[6] for which N_e decreased to 0.7. Anderson and Eaton[3] theorized that the reduction of N_e was related to a nondimensional freestream turning rate defined as the ratio of boundary-layer thickness to the radius of curvature of the freestream streamline (δ/R). The N_e values in the present experiment agreed with the trend that flows with larger nondimensional turning rates experience larger decreases in N_e.

The effect of the turbulence in transporting various quantities in the y direction was expressed as an effective vertical velocity. For the TKE, one can define the following vertical transport velocity:

$$V_{q^2} \equiv (\overline{u^2v} + \overline{v^3} + \overline{vw^2})/\overline{q^2} \tag{8}$$

Note that this quantity nominally tends to 0/0 outside the boundary layer so that values in the outer part of the boundary layer will be scattered. Figure 9 shows that TKE was transported away from the wall by the turbulent fluctuations in the upstream two-dimensional TBL region. At measurement stations in the bend and downstream sections, the transport of TKE was altered. For the measurement elevations closest to the wall, the vertical transport was reduced and eventually reversed direction, whereas it was enhanced in the outer half of the boundary layer. This represents an important change in the physics of the boundary layer. The net downward transport of TKE implies that inactive motions existed and/or that the peak in $\overline{q^2}$ at $y/\delta_{99} \approx 0.3$ led to transport of TKE down the gradient of $\overline{q^2}$.

Turbulent Kinetic Energy Budget

Using the experimental data and the transport equation for the Reynolds stresses

$$U_l(-\overline{u_iu_j})_{,l} = \mathcal{P}_{ij} + \Phi_{ij} - \mathcal{D}_{ij} + \mathcal{J}_{ijk,k} \tag{9}$$

where the generation term $\mathcal{P}_{ij}$, the pressure-strain redistribution term Φ_{ij}, the viscous-destruction term $\mathcal{D}_{ij}$, and the flux of $-\overline{u_iu_j}$ in the x_k direction $\mathcal{J}_{ijk}$ are defined by

$$\mathcal{P}_{ij} \equiv \overline{u_iu_k}U_{j,k} + \overline{u_ju_k}U_{i,k} \tag{10}$$

$$\Phi_{ij} \equiv -(1/\rho)\,\overline{p'(u_{i,j} + u_{j,i})} \tag{11}$$

$$\mathcal{D}_{ij} \equiv 2\nu\overline{u_{i,k}u_{j,k}} \tag{12}$$

$$\mathcal{J}_{ijk} \equiv (1/\rho)(\overline{p'u_i}\delta_{jk} + \overline{p'u_j}\delta_{ik}) + \overline{u_iu_ju_k} + \nu(\overline{u_iu_j})_{,k} \tag{13}$$

one can study the contributions of various physical mechanisms affecting the Reynolds stresses. The measured data allow most of the terms to be evaluated and the other major terms to be deduced by difference. Some terms were not measured because accurate measurements would have been very difficult (dissipation) or because no instrumentation existed to make the measurements (pressure fluctuations).

Seven locations along the centerline of the tunnel were chosen to study the changes occurring in the various terms. At each location, five data set profiles were used to calculate x, y, and z spatial derivatives. Derivatives of mean velocities, Reynolds stresses, and triple products were calculated using central finite differences. Before calculating the derivatives, the data were smoothed in the vertical direction by transforming into Fourier space, low-pass filtering the data, and then performing an inverse Fourier transform. The uncertainties of the terms in the transport equations were essentially the same as the uncertainties of the turbulence statistics from which the transport equation terms were computed. Since the largest gradients were in the y direction, where the data points were closely spaced, and the measured quantities varied smoothly in the x-z plane, the uncertainties due to finite difference approximations were considered small. Arbitrarily, a coordinate system aligned with the local tunnel centerline was used to study the transport.

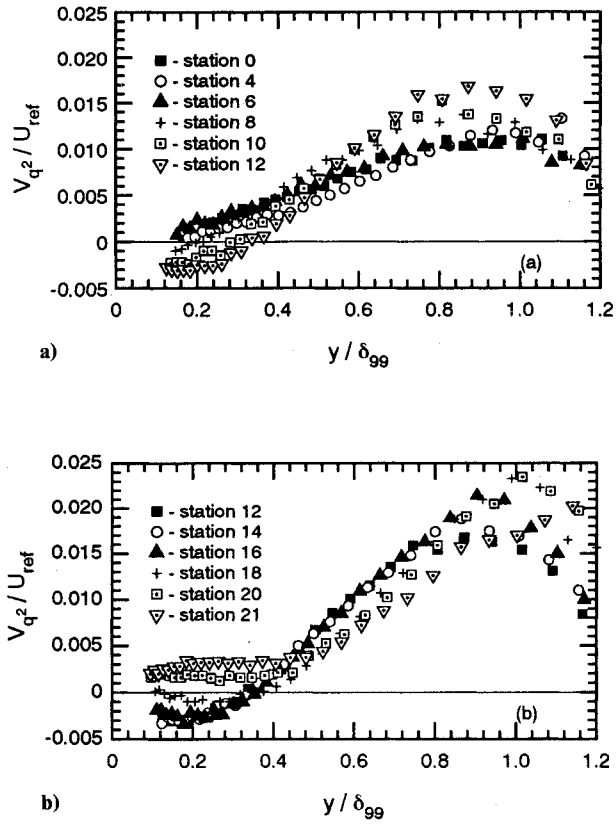

Fig. 9 Vertical transport velocity V_{q^2}: a) crossflow development, b) crossflow decay.

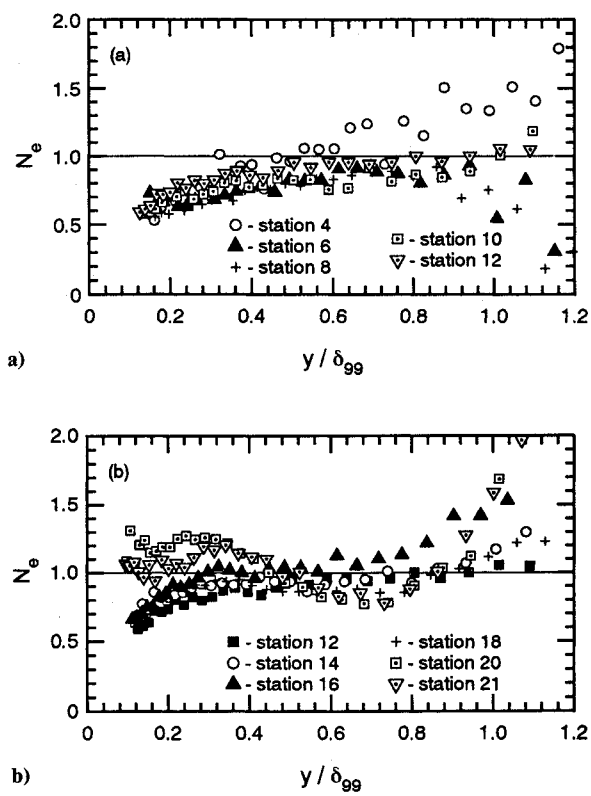

Fig. 8 Profiles of the eddy-viscosity ratio: a) crossflow development, b) crossflow decay.

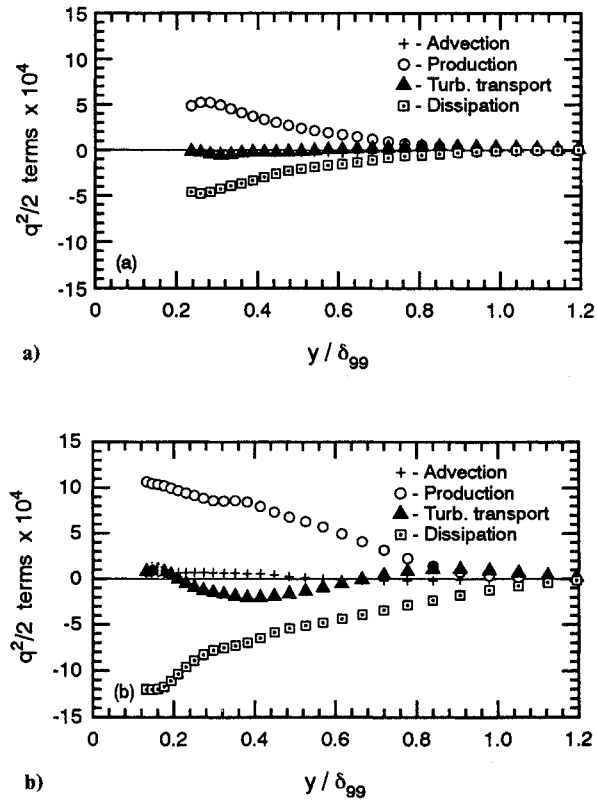

Fig. 10 TKE transport equation terms: a) station 1, b) station 13.

The transport equation for TKE can be written as

$$U_l(\overline{q^2}/2)_{,l} = -\tfrac{1}{2}\,\overline{u_i u_j}U_{i,j} - \tfrac{1}{2}(\overline{u_i u_i u_j})_{,j} + \nu(\overline{q^2}/2)_{,jj} - \nu\overline{u_{i,j}u_{i,j}} - (1/\rho)(\overline{p' u_i}\delta_{il})_{,l} \quad (14)$$

The pressure-diffusion term, not measurable, was assumed small as is done in many closure models. Actually, most models lump it with the triple products and assume proportionality to the Reynolds-stress gradients. The dissipation term was indirectly determined by summing the terms of the equation.

Figure 10a shows the terms in the TKE transport equation at the two-dimensional TBL location $x = 978$ mm (station 1 in Fig. 1). The terms have been nondimensionalized by multiplying by δ/U_{ref}^3 to show relative changes in magnitude. The dissipation term was approximately equal to the production term because of the relatively small size of the advection and turbulent transport terms. Near the edge of the boundary layer, the mean velocity gradient decreased and consequently reduced the production of TKE. The production and dissipation terms approached zero faster than the transport terms. Figure 10b compares the terms in the TKE transport equation for a measurement station where crossflow was large. Again, production was the dominant term, but this time it was due to the mean crossflow velocity gradient $\partial W/\partial y$ in addition to $\partial U/\partial y$. A major difference between the two-dimensional and three-dimensional locations was the increased role of the advection and turbulent transport mechanisms. The transport of TKE due to turbulence was chiefly due to the derivatives in the vertical direction of the triple products meaning x, z turbulent transport was small (boundary-layer approximation).

Conclusions

The development of crossflow affected the turbulence structure of a two-dimensional TBL that was transformed into a three-dimensional TBL via a cross-stream pressure gradient. Measurements using three-hole pressure probes and hot-wire anemometers showed how the boundary layer responded to the crossflow development and subsequent decay.

In the crossflow development region, the mean velocity gradient $\partial W/\partial y$, zero in two-dimensional TBLs, contributed to increased TKE production. Similarly, all three shear components of the Reynolds-stress tensor also increased in magnitude. In the inner half of the boundary layer, the a_1 parameter decreased to approximately 0.12 because the increase in turbulent shear stress was not as large as the TKE increase. The direction of the shear-stress vector lagged behind the direction of the mean velocity-gradient vector as the crossflow developed. This lagging behavior, also observed in other three-dimensional TBL experiments, confirms that the turbulence takes time to react to changes in the mean flowfield and that history effects may be important. Finally, the effective vertical transport of TKE by turbulence was modified by the crossflow development. The transport of TKE was reversed for $y/\delta < 0.4$ and enhanced for $y/\delta > 0.4$. Thus, the flow physics were changed significantly, which suggests the presence of inactive motions inhibiting the normal production of shear stresses.

Immediately downstream of the bend, $\overline{u^2}$ and $-\overline{uv}$ decreased as the turning of the flow ceased, whereas the $-\overline{uw}$ and $-\overline{vw}$ profiles remained unchanged in the slowly decaying crossflow. Further downstream, all of the Reynolds stresses decreased as the boundary layer thickened and the crossflow decayed. In the downstream part of the test section, the a_1 parameter decreased further. The behavior of the a_1 parameter depended on both pressure gradient conditions and the amount of crossflow. The shear-stress and velocity-gradient vectors became nearly aligned again, signifying that the boundary layer was approaching equilibrium.

The present experiment provides new data for developing and testing turbulence models for three-dimensional TBLs. It was designed to produce strong crossflow without the strong streamwise pressure gradients that have complicated the interpretation of previous experiments. The bend applies crossflow in a fairly short streamwise distance, so the flow approximates the response and recovery of an initially two-dimensional TBL to a step increase in longitudinal mean vorticity. The bend angle is sufficiently small that the sidewall boundary layers do not contaminate the floor boundary layer in the test region. Another advance over previous work is that the measurements are detailed enough for all terms in the Reynolds-stress transport equations to be evaluated, either directly or by difference. The complete data set is available from the authors on floppy disk.

Acknowledgments

The authors gratefully acknowledge the support of the Boeing Company under Contract TO-582834-0757N and the support of the Scholarship Foundation of the Society of Experimental Test Pilots. We would also like to thank our colleagues John K. Eaton and James P. Johnston for helpful discussions.

References

[1]Johnston, J. P., "Experimental Studies in Three-Dimensional Turbulent Boundary Layers," Thermosciences Div., Stanford Univ., Rept. MD-34, Stanford, CA, July 1976.

[2]Fernholz, H. H., and Vagt, J. D., "Turbulence Measurements in an Adverse Pressure Gradient Three-Dimensional Turbulent Boundary Layer Along a Circular Cylinder," *Journal of Fluid Mechanics,* Vol. 111, Oct. 1981, pp. 233–269.

[3]Anderson, S. D., and Eaton, J. K., "Reynolds Stress Development in Pressure-Driven Three-Dimensional Turbulent Boundary Layers," *Journal of Fluid Mechanics,* Vol. 202, May 1989, pp. 263–294.

[4]Bradshaw, P., and Terrell, M. G., "The Response of a Turbulent Boundary Layer on an 'Infinite' Swept Wing to the Sudden Removal of Pressure Gradient," National Physical Lab. Aero Rept. 1305, Teddington, England, UK, 1969.

[5]Johnston, J. P., "Measurements in a Three-Dimensional Turbulent Boundary Layer Induced by a Swept, Forward-Facing Step," *Journal of Fluid Mechanics,* Vol. 42, July 1970, pp. 823–844.

[6]Elsenaar, A., and Boelsma, S. H., "Measurements of the Reynolds Stress Tensor in a Three-Dimensional Turbulent Boundary Layer Under Infinite Swept Wing Conditions," National Aerospace Lab., NLR TR 74095 U, Amsterdam, The Netherlands, 1974.

[7]East, L. F., and Sawyer, W. G., "Measurements of the Turbulence Ahead of a 45° Swept Step Using a Double Split-Film Probe," Royal Aircraft Establishment, TR79136, Farnborough, Hampshire, England, UK, 1979.

[8]Bradshaw, P., and Pontikos, N. S., "Measurements in the Turbulent Boundary Layer on an 'Infinite' Swept Wing," *Journal of Fluid Mechanics,* Vol. 159, Oct. 1985, pp. 105–130.

[9]Pierce, F. J., and Duerson, S. H., "Reynolds Stress Tensors in an End-Wall Three-Dimensional Channel Boundary Layer," *Journal of Fluids Engineering,* Vol. 96, Dec. 1975, pp. 61–67.

[10]DeGrande, G., and Hirsch, C., "Three-Dimensional Incompressible Turbulent Boundary Layers," Free Univ. of Brussels, Rept. VUB-STR-8, Brussels, Belgium, Oct. 1978.

[11]Pierce, F. J., and Ezekewe, C. I., "Measured $\overline{uw}$ Stress Gradients in a Three-Dimensional Turbulent Boundary Layer," *Journal of Fluids Engineering,* Vol. 98, Dec. 1976, pp. 768–770.

[12]Dechow, R., and Felsch, K.O., "Measurements of the Mean Velocity and of the Reynolds Stress Tensor in a Three-Dimensional Turbulent Boundary Layer Induced by a Cylinder Standing on a Flat Wall," *Proceedings of 1st International Symposium on Turbulent Shear Flows,* Vol. 1, University Park, PA, April 18–20, 1977.

[13]Müller, U. R., "Measurement of the Reynolds Stresses and the Mean-Flow Field in a Three-Dimensional Pressure-Driven Boundary Layer," *Journal of Fluid Mechanics,* Vol. 119, June 1982, pp. 121–153.

[14]Bissonnette, L. R., and Mellor, G. L., "Experiments on the Behaviour of an Axisymmetric Turbulent Boundary Layer with a Sudden Circumferential Strain," *Journal of Fluid Mechanics,* Vol. 63, Feb. 1974, pp. 369–413.

[15]Lohmann, R. P., "The Response of a Developed Turbulent Boundary Layer to Local Transverse Surface Motion," *Journal of Fluids Engineering,* Vol. 98, Sept. 1976, pp. 355–363.

[16]Driver, D. M., and Hebbar, S. K., "Experimental Study of a Three-Dimensional, Shear-Driven, Turbulent Boundary Layer," *AIAA Journal,* Vol. 25, No. 1, 1987, pp. 35–42.

[17]Driver, D. M., and Johnston, J.P., "Experimental Study of a Three-Dimensional Shear-Driven Turbulent Boundary Layer with Streamwise Adverse Pressure Gradient," NASA TM 102211, May 1990.

[18]Littell, H. S., and Eaton, J. K., "An Experimental Investigation of the Three-Dimensional Boundary Layer on a Rotating Disk," Thermosciences Div., Stanford Univ., Rept. MD-60, Stanford, CA, Dec. 1991.

[19]Spalart, P. R., "Theoretical and Numerical Study of a Three-Dimensional Turbulent Boundary Layer," *Journal of Fluid Mechanics,* Vol. 205, Aug. 1989, pp. 319–340.

[20]Moin, P., Shih, T. H., Driver, D., and Mansour, N. M., "Direct Numerical Simulation of a Three-Dimensional Turbulent Boundary Layer," *Physics of Fluids A,* Vol. 2, No. 10, 1990, pp.1846–1853.

[21]Sendstad, O., and Moin, P., "The Near Wall Mechanics of Three-Dimensional Turbulent Boundary Layers," Thermosciences Div., Stanford Univ., Rept. TF–57, Stanford, CA, Dec. 1992.

[22]Eaton, J. K., "Turbulence Structure and Heat Transfer in Three-Dimensional Boundary Layers," 9th Symposium on Energy Engineering Sciences, Argonne National Lab., 1991.

[23]Schwarz, W. R., and Bradshaw, P., "Three-Dimensional Turbulent Boundary Layer in a 30 Degree Bend: Experiment and Modelling," Thermosciences Div., Stanford Univ., Rept. MD-61, Stanford, CA, Oct. 1992.

[24]Flack, K. A., and Johnston, J. P., "Near-Wall Turbulent Flows," *Proceedings of the International Conference on Near-Wall Turbulent Flows,* Tempe, AZ, March 15–17, 1993, pp. 977–986.

[25]Bryer, D.W., and Pankhurst, R.C., *Pressure-Probe Methods for Determining Wind Speed and Flow Direction,* Her Majesty's Stationery Office, London, 1971.

[26]Young, A. D., and Maas, J. N., "The Behavior of a Pitot Tube in a Transverse Total-Pressure Gradient," Aeronautical Research Council, Rept. 1770, London, England, UK, 1936.

[27]Patel, V. C., "Calibration of the Preston Tube and Limitations on Its Use in Pressure Gradients," *Journal of Fluid Mechanics,* Vol. 23, Jan. 1965, pp. 185–208.

[28]Pierce, F. J., McAllister, J. E., and Tennant, M. H., "Near-Wall Similarity in a Pressure-Driven Three-Dimensional Turbulent Boundary Layer," *Journal of Fluids Engineering,* Vol. 105, Sept. 1983, pp. 257–262.

[29]Degani, A. T., Smith, F. T., and Walker, J. D. A., "The Three-Dimensional Turbulent Boundary Layer Near a Plane of Symmetry," *Journal of Fluid Mechanics,* Vol. 234, 1992, pp. 329–360.

[30]Bearman, P. W., "Corrections for the Effect of Ambient Temperature Drift on Hot-Wire Measurements in Incompressible Flow," DISA Electronics, Rept. 11, Franklin Lakes, NJ, May 1971, pp. 25–30.

[31]Klebanoff, P. S., "Characteristics of Turbulence in a Boundary Layer with Zero Pressure Gradient," NACA TN3178, July 1954.

[32]Murlis, J., Tsai, H. M., and Bradshaw, P., "The Structure of Turbulent Boundary Layers at Low Reynolds Numbers," *Journal of Fluid Mechanics,* Vol. 122, Sept. 1982, pp. 13–56.

[33]Kays, W.M. and Crawford, M.E., *Convective Heat and Mass Transfer,* 2nd ed., McGraw-Hill, New York, 1980, p.174.

[34]Squire, H. B. and Winter, K. G., "The Secondary Flow in a Cascade of Airfoils in a Nonuniform Stream," *Journal of the Aeronautical Sciences,* Vol. 18, No. 4, 1951, pp.271–277.

[35]Hawthorne, W. R., "Secondary Circulation in Fluid Flow," *Proceedings of the Royal Society of London Series A: Mathematical and Physical Sciences,* Vol. 206, 1951, p. 374.

[36]Bradshaw, P., "The Turbulence Structure of Equilibrium Boundary Layers," *Journal of Fluid Mechanics,* Vol. 29, Pt. 4, 1967, pp. 625–645.